

Article

Chain Compounds Based on Paddle-wheel Copper(II) Carboxylate Bearing Four Nitroxide Radicals

Masahiro Mikuriya ^{1,*} , Renny Indrawati ¹ , Rieko Hashido ¹, Shizuka Matsubara ¹, Chizu Nakamura ¹, Daisuke Yoshioka ¹, Kazuyuki Yokota ¹, Masafumi Fukuzaki ¹ and Makoto Handa ²

¹ Department of Applied Chemistry for Environment and Reserach Center for Coordination Molecule-Based Devices, School of Science and Technology, Kwansei Gakuin University, 2-1 Gakuen, Sanda 669-1337, Japan; renny_indrawati@yahoo.com (R.I.); hashido.rieko@gmail.com (R.H.); shizukanet@docomo.ne.jp (S.M.); chizu0904@gmail.com (C.N.); yoshi0431@gmail.com (D.Y.); endless_7@hotmail.co.jp (K.Y.); fukuzakimasafumi@yahoo.co.jp (M.F.)

² Department of Chemistry, Interdisciplinary Graduate School of Science and Engineering, Shimane University, Matsue 690-8504, Japan; handam@riko.shimane-u.ac.jp

* Correspondence: junpei@kwansei.ac.jp; Tel.: +81-79-565-8365

Received: 18 April 2018; Accepted: 7 May 2018; Published: 10 May 2018



Abstract: Chain compounds of paddle-wheel Cu₂-clusters of 3-carboxy-2,2,5,5-tetramethyl-1-pyrrolidinyloxy (Hcaproxy) and 4-carboxy-2,2,6,6-tetramethylpiperidinyloxy (Hcatempo) and *N,N'*-bidentate ligands (L = 4,4'-bipyridine (4,4'-bpy), 1,2-bis(4-pyridyl)ethane (bpe), *trans*-1,2-bis(4-pyridyl)ethylene (bpel), 4,4'-dipyridyl disulfide (pds), 1,4-diazabicyclo[2.2.2]octane (dabco), and pyrazine (pyz)), [Cu₂(caproxy)₄(L)]_n, and [Cu₂(catempo)₄(L)]_n, were synthesized and characterized by elemental analysis, infrared and UV-vis spectra and temperature dependence of magnetic susceptibilities (4.5–300 K). The crystal structures of [Cu₂(caproxy)₄(pds)]_n, [Cu₂(catempo)₄(4,4'-bpy)]_n, and [Cu₂(catempo)₄(bpe)]_n revealed zigzag or linear chains consisting of alternate arrangement of the dinuclear cluster bearing four nitroxide radicals and *N,N'*-bidentate ligand. Temperature dependence of magnetic susceptibilities showed a considerable antiferromagnetic interaction between the two copper(II) ions within the dinuclear cluster, and weak antiferromagnetic interaction between the dinuclear clusters and/or the radical and dinuclear cluster.

Keywords: copper(II) carboxylate; organic radical; nitroxide radical; chain compound; antiferromagnetic interaction

1. Introduction

Copper acetate is one of the old-fashioned metal complexes with a paddle-wheel-like or lantern-like cluster and has attracted much attention since the discovery of the unique dinuclear structure with antiferromagnetic spin-coupling [1–7]. We have engaged in the synthesis of copper acetate analogues and their coordination polymer complexes [8–24]. Previously, we reported that a chain compound of copper(II) benzoate with pyrazine shows an adsorption property for N₂ because of the hydrophobic micropore that is formed by the aromatic benzoate groups [12,24]. This is an interesting feature of this type of coordination polymers. In order to extend copper acetate analogues, we introduced some organic radicals to copper(II) propionate to make adducts with organic radicals, by using pyridyl nitronyl nitroxides [14]. Similar studies on copper acetate type complexes with pyridyl nitronyl nitroxides were reported by Wei et al. [25,26], Ouahab et al. [27], and Miller et al. [28]. We also prepared copper acetate analogues with free radical carboxylic acids, 4-carboxy-2,2,6,6-tetramethylpiperidinyloxy

(Hcatempo), and 3-carboxy-2,2,5,5-tetramethyl-1-pyrrolidinyloxy (Hcaproxy) (Figure 1) [18]. In order to construct new coordination polymers with an interesting structures and properties, we combined these copper acetate type units and N,N' -bidentate linking ligands, 4,4'-bipyridine (4,4'-bpy), 1,2-bis(4-pyridyl)ethane (bpe), *trans*-1,2-bis(4-pyridyl)ethylene (bpel), 4,4'-dipyridyl disulfide (pds), and 1,4-diazabicyclo[2.2.2]octane (dabco), and pyrazine (pyz), aiming at chain compounds that are shown in Figure 2. Among the present linking ligands, the pds ligand is interesting, having a twisted structure and accompanying the axial chirality with the *P*- and the *M*-forms of optical antipodes [19]. We report here on the synthesis, magnetic properties, and crystal structures of these coordination polymers.

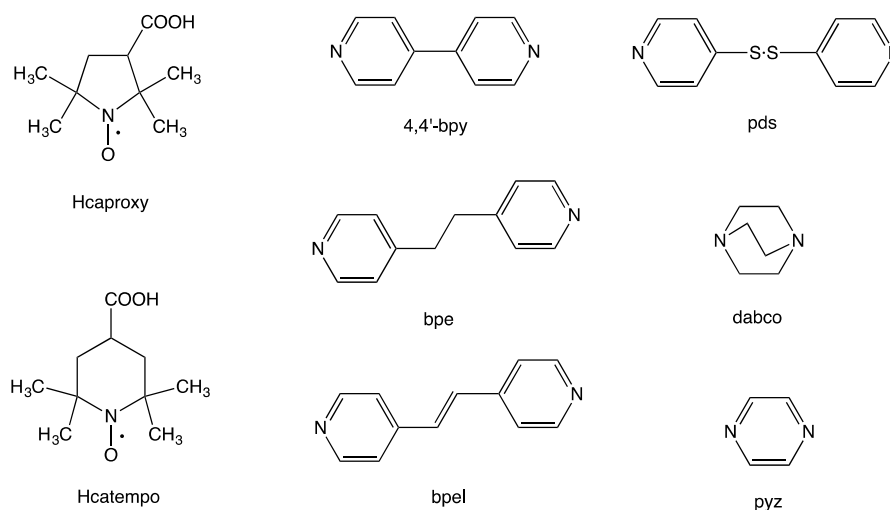


Figure 1. Free radical carboxylic acids, 3-carboxy-2,2,5,5-tetramethyl-1-pyrrolidinyloxy (Hcaproxy) and 4-carboxy-2,2,6,6-tetramethylpiperidinyloxy (Hcatempo), and linking N,N' -bidentate ligands, 4,4'-bipyridine (4,4'-bpy), 1,2-bis(4-pyridyl)ethane (bpe), *trans*-1,2-bis(4-pyridyl)ethylene (bpel), 4,4'-dipyridyl disulfide (pds), 1,4-diazabicyclo[2.2.2]octane (dabco), and pyrazine (pyz)).

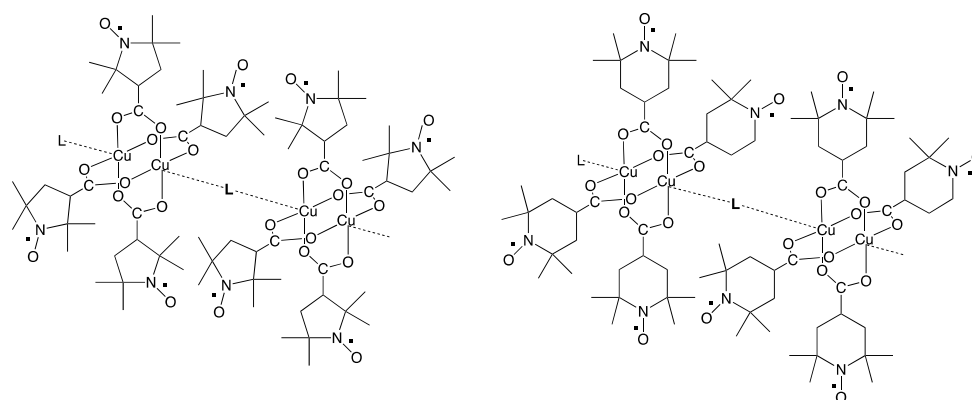


Figure 2. Chain compounds of Cu₂(caproxy)₄ and Cu₂(catempo)₄ with N,N' -bidentate ligands, L.

2. Results and Discussion

2.1. Synthesis of Chain Compounds

The parent dinuclear copper(II) carboxylates, [Cu₂(caproxy)₄(H₂O)₂] (1), and [Cu₂(catempo)₄(H₂O)₂] (2), were synthesized, according to the previously reported method [18]. Reaction of the parent dinuclear copper(II) carboxylate and linking ligand formed coordination polymers with a one-dimensional chain structure: [Cu₂(caproxy)₄(4,4'-bpy)]_n (3), [Cu₂(caproxy)₄(bpe)]_n

(4), $[\text{Cu}_2(\text{caproxy})_4(\text{bpel})]_n$ (5), $[\text{Cu}_2(\text{caproxy})_4(\text{pds})]_n$ (6), $[\text{Cu}_2(\text{caproxy})_4(\text{dabco})]_n$ (7), $[\text{Cu}_2(\text{caproxy})_4(\text{pyz})]_n$ (8), $[\text{Cu}_2(\text{catempo})_4(4,4'\text{-bpy})]_n$ (9), $[\text{Cu}_2(\text{catempo})_4(\text{bpe})]_n$ (10), $[\text{Cu}_2(\text{catempo})_4(\text{bpel})]_n$ (11), $[\text{Cu}_2(\text{catempo})_4(\text{pds})]_n$ (12), and $[\text{Cu}_2(\text{catempo})_4(\text{dabco})]_n$ (13). Elemental analysis data of the isolated compounds are in accordance with the formulation of these coordination polymers. Many trials to prepare the chain adduct of catempo system with pyrazine were unsuccessful, resulting in recovery of the parent complex, which was confirmed by elemental analysis and infrared spectra.

2.2. Infrared Spectra of Chain Compounds

Infrared spectra of the chain compound **3** are compared with those of the parent dinuclear copper(II) complex **1** in Figure 3 as a representative example. Infrared spectral data of all of the present compounds are listed in Tables 1 and 2. The present compounds showed two COO stretching bands at 1609–1635 and 1398–1423 cm^{-1} , with the difference in energy characteristic of *syn-syn*-bridging carboxylate as similar to the parent dinuclear copper(II) complexes, showing the preserved structure of the paddle-wheel-like dinuclear core in the chain compounds [29]. The NO stretching band due to the nitroxide moiety was observed at 1361–1365 cm^{-1} , as similar to the parent dinuclear copper(II) complexes, showing the presence of the nitroxide radicals. The medium band at around 1009–1074 cm^{-1} can be assigned as the pyridine ring-breathing modes, suggesting the presence of the pyridine-containing linking ligands in the compounds **3–6** and **9–12** [30]. It is known that the shift of the pyridine ring vibrational band (ν (CC/CN)) to the higher energy side is indicative of the coordination of the pyridine nitrogen atom to metal ion [31–33]. The corresponding vibration of free 4,4'-bpy, bpe, bpel, and pds could be observed as a strong band at 1597, 1596, 1596, and 1574 cm^{-1} , respectively. These vibration bands tend to be shifted to a higher energy region in most of the chain compounds, suggesting the coordination of the linking ligand to the dinuclear cluster. In the infrared spectra of **7** and **13**, two medium bands corresponding to the skeletal modes of dabco molecule [34] can be found, suggesting the presence of dabco ligand in these compounds.

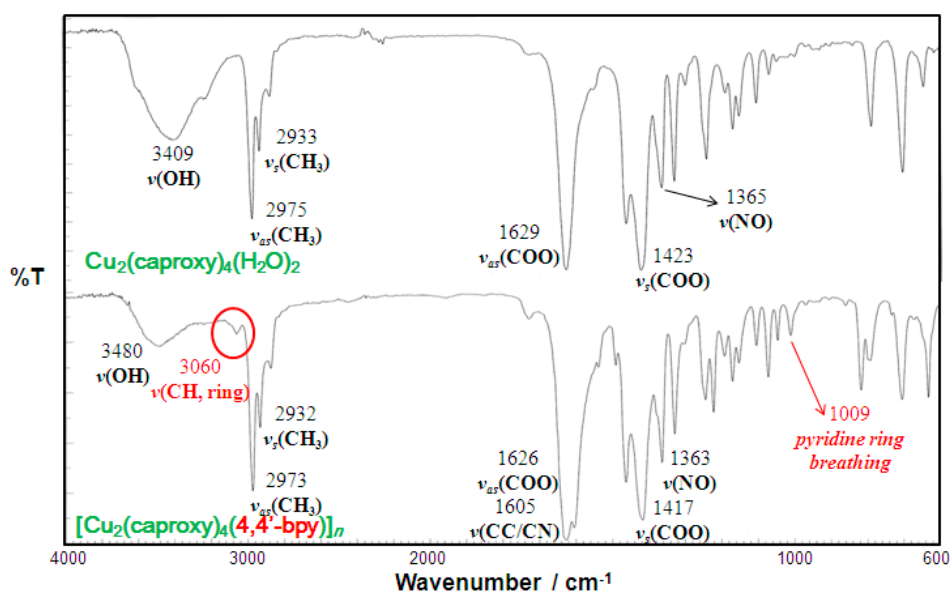


Figure 3. Infrared spectra of $[\text{Cu}_2(\text{caproxy})_4(4,4'\text{-bpy})]_n$ (**3**) compared with those of the parent compound (**1**).

Table 1. Infrared spectral data of $[\text{Cu}_2(\text{caproxy})_4(\text{H}_2\text{O})_2]$ (1) and chain compounds $[\text{Cu}_2(\text{caproxy})_4(\text{L})]_n$ L = 4,4'-bpy (3), bpe (4), bpeI (5), pds (6), dabco (7), and pyz (8).

$[\text{Cu}_2(\text{caproxy})_4(\text{H}_2\text{O})_2]$ (1)	$[\text{Cu}_2(\text{caproxy})_4(\text{L})]_n$ ^a						Assignment
	4,4'-bpy (3)	bpe (4)	bpeI (5)	pds (6)	dabco (7)	pyz (8)	
3409(mbr)	3480(wbr)	3469(wbr)	3507(wbr)	3475(wbr)	3494(wbr)	3439(wbr)	$\nu(\text{OH})$
-	3060(vw)	3064(vw)	3056(vw)	3057(vw)	-	3103(vw)	$\nu(\text{CH, ring})$
2975(s)	2973(s)	2971(s)	2973(s)	2973(s)	2974(s)	2974(s)	$\nu_{as}(\text{CH}_3)$
2933(m)	2932(m)	2930(m)	2931(m)	2931(m)	2932(m)	2933(m)	$\nu_s(\text{CH}_3)$
1629(vs)	1626(vs)	1609(vs)	1628(vs)	1628(vs)	1625(vs)	1620(vs)	$\nu_{as}(\text{COO})$
1423(vs)	1417(vs)	1403(s)	1423(vs)	1417(vs)	1422(s)	1419(vs)	$\nu_s(\text{COO})$
206	209	206	205	211	203	201	$\Delta\nu(\text{COO})$ ^b
-	1605(vs)	1576(vs)	1607(vs)	1585(vs)	-	-	$\nu(\text{CC/CN})$
1365(s)	1363(s)	1362(s)	1363(s)	1362(s)	1362(s)	1362(s)	$\nu(\text{NO})$
-	1009(w)	1036(m)	1018(m)	1032(w)	-	-	pyridine ring breathing
-	-	-	-	-	1058, 1004(m)	-	skeletal mode
-	-	-	-	-	-	813(m)	CH out-of-plane

^a vs, very strong; s, strong; m, medium; w, weak; vw, very weak; br, broad; ν_{as} , antisymmetric stretching; ν_s , symmetric stretching. ^b $\Delta\nu(\text{COO}) = \nu_{as}(\text{COO}) - \nu_s(\text{COO})$.

Table 2. Infrared spectral data of $[\text{Cu}_2(\text{catempo})_4(\text{H}_2\text{O})_2]$ (2) and chain compounds $[\text{Cu}_2(\text{catempo})_4(\text{L})]_n$ L = 4,4'-bpy (9), bpe (10), bpeI (11), pds (12), and dabco (13).

$[\text{Cu}_2(\text{catempo})_4(\text{H}_2\text{O})_2]$ (2)	$[\text{Cu}_2(\text{catempo})_4(\text{L})]_n$ ^a					Assignment
	4,4'-bpy (9)	bpe (10)	bpeI (11)	pds (12)	dabco (13)	
3419(sbr)	-	3442(vwbr)	3501(mbr)	3484(wbr)	3481(wbr)	$\nu(\text{OH})$
-	3061(vw)	3053(vw)	3046(vw)	3099(vw)	-	$\nu(\text{CH, ring})$
2973(vs)	2976(s)	2974(s)	2974(m)	2972(s)	2977(m)	$\nu_{as}(\text{CH}_3)$
2934(s)	2935(m)	2934(m)	2925(m)	2936(s)	2939(m)	$\nu_s(\text{CH}_3)$
1635(vs)	1627(vs)	1627(vs)	1613(vs)	1626(vs)	1625(vs)	$\nu_{as}(\text{COO})$
1417(vs)	1416(vs)	1415(vs)	1398(s)	1416(vs)	1418(s)	$\nu_s(\text{COO})$
218	211	212	215	210	207	$\Delta\nu(\text{COO})$ ^b
-	1604(vs)	1612(vs)	(1613)(vs)	1590(vs)	-	$\nu(\text{CC/CN})$
1364(s)	1361(m)	1361(s)	1361(m)	1361(s)	1361(m)	$\nu(\text{NO})$
-	1074(w)	1018(m)	1029(m)	1065(m)	-	pyridine ring breathing
-	-	-	-	-	1057, 1004(w)	skeletal mode

^a vs, very strong; s, strong; m, medium; w, weak; vw, very weak; br, broad; ν_{as} , antisymmetric stretching; ν_s , symmetric stretching. ^b $\Delta\nu(\text{COO}) = \nu_{as}(\text{COO}) - \nu_s(\text{COO})$.

2.3. Electronic Spectra of Chain Compounds

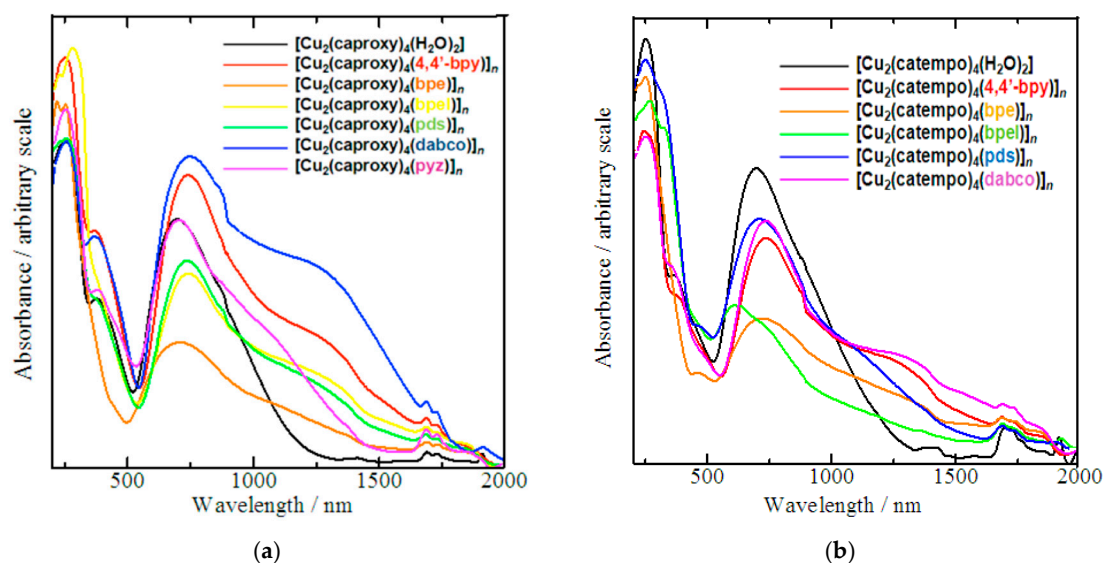
The absorption bands that were observed in the electronic spectra of compounds 1–13 are listed in Tables 3 and 4. The diffused reflectance spectra of all the compounds (Figure 4) can be characterized as three main absorption bands, as previously reported for copper(II) acetate type cluster systems [5,7]. The ligand to metal charge transfer is responsible for the high intensity bands in the UV region. The shoulder-like absorption band at near-UV region can be assumed as a characteristic band of copper(II) acetate type clusters [5,7]. Furthermore, all broad bands spanned in the visible and NIR regions until around 1000 nm are typically interpreted as d-d transitions [35]. Although these main absorption bands appear at almost the same region, the d-d transition bands of the chain compounds have more clear shoulder band at lower energy side compared with those of the parent complexes, reflecting the coordination of the N,N' -bidentate ligand in the chain compounds. The comparatively strong σ -electron donation of the axial nitrogen donor than the oxygen donor of the aqua ligand of the parent compounds may explain this difference [35]. Methanol solutions of these complexes show an intense UV-band with λ_{max} at 205–225 nm ($\epsilon \approx 2820\text{--}12030 \text{ mol}^{-1} \text{ dm}^3 \text{ cm}^{-1}$), which might be ascribed to ligand-to-metal charge transfer (LMCT). The broad absorption band at Vis-NIR region with λ_{max} centered around 700 nm ($\epsilon \approx 110\text{--}340 \text{ mol}^{-1} \text{ dm}^3 \text{ cm}^{-1}$) can be assigned to the characteristic copper(II) d-d transitions [35]. Despite those transition bands, the expected absorption for the copper acetate type clusters may be superimposed with the nearest LMCT band. We occasionally detected a vague shouldering band at around 370 nm.

Table 3. Electronic spectral data of $[\text{Cu}_2(\text{caproxy})_4(\text{H}_2\text{O})_2]$ (1) and chain compounds $[\text{Cu}_2(\text{caproxy})_4(\text{L})]_n$ L = 4,4'-bpy (3), bpe (4), bpeI (5), pds (6), dabco (7), and pyz (8).

	1	Chain Compound (Linking Ligand)					
		3 (4,4'-bpy)	4 (bpe)	5 (bpeI)	6 (pds)	7 (dabco)	8 (pyz)
λ_{max} (nm); [$\epsilon \times 10^3$, $\text{mol}^{-1} \text{dm}^3 \text{cm}^{-1}$] (methanol solution)	205 [3.47] 703 [0.34]	208 [5.68] 703 [0.31]	206 [7.10] 700 [0.22]	209 [8.20] 703 [0.29]	225 [10.35] 702 [0.26]	207 [7.20] 702 [0.25]	209 [7.18] 705 [0.33]
λ_{max} (nm); (solid-state, diffused reflectance) ^a	254 378(sh) 699(br)	253 366(sh) 739(br)	219 253(sh) 707(br)	226(sh) 283 741(br)	258 382(sh) 737(br)	257 366(sh) 746(br)	255 380(sh) 703(br)

^a sh, shoulder; br, broad.**Table 4.** Electronic spectral data of $[\text{Cu}_2(\text{catempo})_4(\text{H}_2\text{O})_2]$ (2) and chain compounds $[\text{Cu}_2(\text{catempo})_4(\text{L})]_n$ L = 4,4'-bpy (9), bpe (10), bpeI (11), pds (12), and dabco (13).

	2	Chain Compound (Linking Ligand) ^a				
		9 (4,4'-bpy)	10 (bpe)	11 (bpeI)	12 (pds)	13 (dabco)
λ_{max} (nm); [$\epsilon \times 10^3$, $\text{mol}^{-1} \text{dm}^3 \text{cm}^{-1}$] (methanol solution)	211 [2.82] 701 [0.16]	210 [8.44] 707 [0.19]	208 [6.16] 708 [0.17]	208 [12.03] 704 [0.11]	205 [6.22] 708 [0.15]	205 [5.89] 705 [0.19]
λ_{max} (nm); (solid-state, diffused reflectance) ^a	252 366(sh) 696(br)	246 380(sh) 736(br)	250 462(sh) 720(br)	269 325(sh) 610(br)	248 332(sh) 708(br)	252 362(sh) 736(br)

^a sh, shoulder; br, broad.**Figure 4.** Diffused reflectance spectra of chain compounds (a) $[\text{Cu}_2(\text{caproxy})_4(\text{L})]_n$ and (b) $[\text{Cu}_2(\text{catempo})_4(\text{L})]_n$.

2.4. Crystal Structures of Chain Compounds

Single crystals suitable for X-ray diffraction work were obtained for the parent dinuclear complex $[\text{Cu}_2(\text{catempo})_4(\text{H}_2\text{O})_2]$ (2). In this study, we obtained better data with good quality crystals, as compared with the previously reported data [18]. Crystal data and details concerning data collection are given in Table 5. Selected bond lengths and angles are listed in Table 6. The crystal and molecular structure of 2 is almost the same as the reported one [18], as shown in Figure 5. The molecule

has a copper acetate type dinuclear core with four catempo[−] carboxylato-bridges, which has a crystallographic inversion center at the mid-point of the Cu₂ core. The axial position of each copper atom is occupied by the water molecule, forming an elongated square-pyramidal geometry. The copper atoms lie on the basal O₄ plane toward the axial nitrogen atom by 0.18 Å. The Cu⋯Cu' distance is 2.6018(4) Å. This feature is normal as the copper acetate type clusters [3–7]. The N1-O3 and N2-O6 bond distances of the catempo[−] moieties are 1.2825(17) and 1.2879(15) Å, respectively, which is comparable to that of tempo radical (1.283(9) Å) [36], showing a normal distance as a free nitroxide radical.

Table 5. Crystallographic data for **2**, **6**, **9**, and **10**.

Complex	2	6	9	10
Empirical formula	C ₄₈ H ₈₄ Cu ₂ N ₈ O ₁₄	C ₄₈ H ₇₄ Cu ₂ N ₇ O _{13.5} S ₂	C ₅₂ H ₈₂ Cu ₂ N ₆ O ₁₄	C ₅₂ H ₈₄ Cu ₂ N ₆ O ₂₀
Formula weight	1124.31	1156.34	1142.31	1240.33
Temperature/K	90	90	293	90
Crystal dimensions/mm	0.30 × 0.35 × 0.45	0.08 × 0.15 × 0.35	0.20 × 0.10 × 0.10	0.60 × 0.35 × 0.10
Crystal system	monoclinic	triclinic	monoclinic	tetragonal
Space group	P2 ₁ /n	P $\bar{1}$	C2/c	I4/mmm
a/Å	15.3355(13)	12.4788(16)	24.463(7)	15.647(2)
b/Å	11.1387(9)	13.0993(17)	13.154(4)	15.647(2)
c/Å	16.7641(14)	21.147(3)	21.260(6)	16.178(3)
α/°	90	98.358(2)	90	90
β/°	90.9100(10)	98.274(2)	107.717(4)	90
γ/°	90	114.674(2)	90	90
V/Å ³	2863.2(4)	3026.3(7)	6517(3)	3960.8(14)
Z	2	2	4	2
d _{calcd.} /gcm ^{−3}	1.304	1.269	1.164	1.040
μ/mm ^{−1}	0.809	0.833	0.711	0.595
F(000)	1196	1218	2424	1312
Reflections collected	18,133	19,461	20,035	12,666
Independent reflections	6897	13,811	7832	1428
θ range for data collection	1.79 to 28.92°	1.76 to 28.53°	1.75 to 28.51°	1.81 to 28.53
Data/Restraints/Parameters	6897/0/341	13811/1/491	7832/0/394	1428/0/143
R1, wR2 [I > 2σ(I)] ^a	0.0303, 0.0772	0.1164, 0.2955	0.0773, 0.1824	0.0895, 0.2536
R1, wR2 (all data) ^a	0.0368, 0.0799	0.2277, 0.3258	0.1927, 0.2325	0.0983, 0.2627
Goodness-of-fit on F ²	1.052	1.397	0.950	1.182
CCDC number	1,836,763	1,836,764	1,836,765	1,836,862

$$^a R1 = \sum | |F_o| - |F_c| | / \sum |F_o|; wR2 = [\sum w(F_o^2 - F_c^2)^2 / \sum w(F_o^2)^2]^{1/2}.$$

Table 6. Selected bond distances (Å) and angles (°), with esds in parentheses for **2**, **6**, **9**, and **10**.

2			
Cu1⋯Cu1'	2.6018(4)	O1-C1	1.2557(17)
Cu1-O1	1.9559(10)	O2-C1	1.2611(17)
Cu1-O2'	1.9682(10)	O4-C11	1.2609(17)
Cu1-O4	1.9767(10)	O5-C11	1.2577(17)
Cu1-O5'	1.9707(10)	N1-O3	1.2825(17)
Cu1-O7	2.1223(11)	N2-O6	1.2879(15)
O1-Cu1-O2'	169.44(4)	O2'-Cu1-O5'	89.33(5)
O1-Cu1-O4	89.30(5)	O2'-Cu1-O7	95.93(5)
O1-Cu1-O5'	90.33(5)	O4-Cu1-O5'	169.45(4)
O1-Cu1-O7	94.61(5)	O4-Cu1-O7	95.09(4)
O2'-Cu1-O4	89.10(5)	O5'-Cu1-O7	95.45(4)

Table 6. Cont.

6			
Cu1...Cu1'	2.6541(19)	Cu2...Cu2''	2.6494(18)
Cu1-O1	1.970(5)	Cu2-O7	1.932(6)
Cu1-O2'	1.957(6)	Cu2-O8''	1.963(6)
Cu1-O4	1.934(6)	Cu2-O10	1.945(6)
Cu1-O5'	1.944(5)	Cu2-O11''	1.947(7)
Cu1-N5	2.165(6)	Cu2-N6	2.144(6)
S1-S2	2.027(4)		
Cu1'...Cu1-N5	174.38(17)	Cu2''...Cu2-N6	176.81(19)
C39-S1-S2	105.0(3)	C44-S2-S1	105.3(3)
9			
Cu1...Cu1'	2.6114(12)	Cu1-O4	1.964(4)
Cu1-O1	1.945(4)	Cu1-O5'	1.959(4)
Cu1-O2'	1.963(4)	Cu1-N3	2.121(4)
Cu1'...Cu1-N3	176.34(12)		
10			
Cu1...Cu1'	2.6115(18)	Cu1-N2	2.112(8)
Cu1-O1	1.965(4)		
Cu1'...Cu1-N2	180.0		

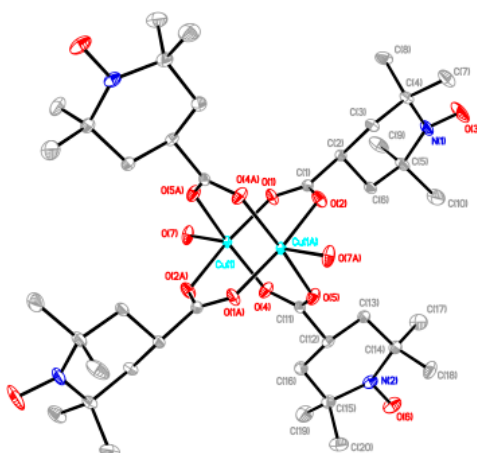


Figure 5. Perspective view of $[\text{Cu}_2(\text{catempo})_4(\text{H}_2\text{O})_2]$ (**2**). Hydrogen atoms are omitted for clarity.

Most of the chain compounds were obtained as microcrystalline precipitates, which are not suitable for single-crystal X-ray analysis. We barely isolated small crystals of **6**, **9**, and **10** after many trials to grow single crystals. Although the qualities of these crystals were not good enough to obtain the precise crystal structures, we could see the chain structures with alternating arrangement of the dinuclear carboxylate cluster and the linking ligand. The chain adduct of $\text{Cu}_2(\text{caproxy})_4$ system with pds ligand, $[\text{Cu}_2(\text{caproxy})_4(\text{pds})]_n$ (**6**), crystallizes in the triclinic system. A perspective view of the crystal structure of compound **6** is shown in Figure 6. The chain molecule consists of alternating linking of dinuclear $\text{Cu}_2(\text{caproxy})_4$ cluster and pds ligand to construct a zigzag chain molecule. There are two crystallographically independent dinuclear $\text{Cu}_2(\text{caproxy})_4$ clusters, of which both have the crystallographic inversion centers at the midpoints of $\text{Cu1}\cdots\text{Cu1}'$ and $\text{Cu2}\cdots\text{Cu2}''$. The $\text{Cu1}\cdots\text{Cu1}'$ and $\text{Cu2}\cdots\text{Cu2}''$ distances are 2.6541(19) and 2.6494(18) Å, respectively. Both of the copper atoms are coordinated by a four carboxylato oxygen atoms of caproxy[−] and pyridyl nitrogen atom of pds with Cu-O distances of 1.932(6)–1.970(5) Å and Cu-N distances of 2.144(6) and 2.165(6) Å, respectively, to form a distorted square pyramidal geometry. This feature is originated from the Jahn-Teller distortion of copper(II) ion and has been similarly observed in several related chain compounds of copper(II) carboxylate groups [10,12,19,21,22]. The copper atom lies on the

basal O_4 plane toward the axial nitrogen atom by 0.20 \AA for Cu1 and Cu2. As our expectation, the pds ligand being a bidentate ligand resulted in the formation of one-dimensional coordination polymer, although the chain is achiral. In view of the fact that the $Cu1'-Cu1-N5$, $C39-S1-S2$, $S1-S2-C44$, and $N6-Cu2-Cu2''$ are $174.38(17)$, $105.0(3)$, $105.3(3)$, and $176.81(19)^\circ$, respectively, it is clear that the structural twisting and bending are escorted by the pds ligand, and thus, this complex has a zig-zag chain feature. The S–S bond distance that is found in the present complex is $2.027(4) \text{ \AA}$. Additionally, the C–S–S–C torsion angle of this pds complex is 94.55° and within the range of torsion angles (78.0 – 96.5°) for various pds metal complexes $[Cu_4(CH_3COO)_6(\mu_3-OH)_2(pds)_2]_n$, $[Cu(CH_3COO)_2(pds)\cdot 6H_2O]_n$, $[\{Cu_2(C_6H_5COO)_4\}_2(pds)_2]_n$, $[\{Cu_2[CH_3(CH_2)_4COO]_4\}_2(pds)_2]_n$, $[Mn(hfac)_2(pds)]_n$, and $[ZnX_2(pds)_2]_n$ ($X = SCN^-$, ClO_4^- , NO_3^-) [19,37,38]. In the crystal, acetonitrile and water molecules are included and hydrogen-bonding are formed between these molecules as shown in Figure 7. We used a racemic mixture of pds ligand and isolated the chain compounds containing the racemic components of pds.

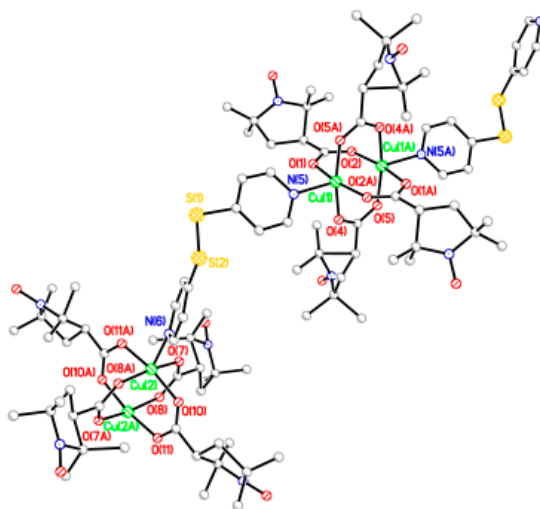


Figure 6. Perspective view of chain molecule for $[Cu_2(\text{caproxy})_4(\text{pds})]_n$ (6). Hydrogen atoms are omitted for clarity.

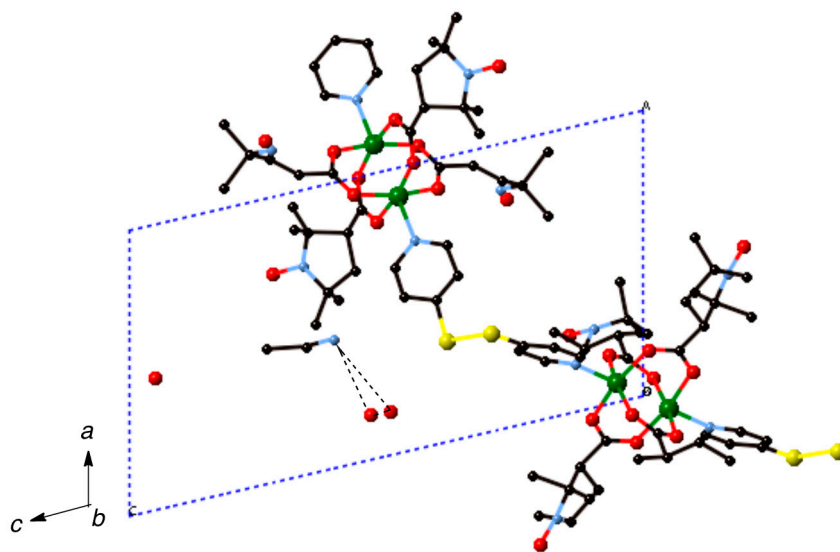


Figure 7. Packing diagram of $[Cu_2(\text{caproxy})_4(\text{pds})]_n$ (6). Hydrogen atoms are omitted for clarity. Dotted lines denote the hydrogen bondings.

The chain adduct of $\text{Cu}_2(\text{catempo})_4$ system with 4,4'-bpy ligand, $[\text{Cu}_2(\text{catempo})_4(4,4'\text{-bpy})]_n$ (**9**), crystallizes in the monoclinic system. A perspective view of the molecular structure of compound **9** is shown in Figure 8. The molecular structure of compound **9** consists of alternating linking of dinuclear $\text{Cu}_2(\text{catempo})_4$ cluster and 4,4'-bpy ligand to construct a nearly-linear chain molecule. There is a crystallographically independent dinuclear $\text{Cu}_2(\text{catempo})_4$ cluster, which has the crystallographic inversion center at the midpoint of $\text{Cu1}\cdots\text{Cu1}'$. The $\text{Cu1}\cdots\text{Cu1}'$ distance is 2.6114(12) Å. The copper atom is coordinated by four carboxylato oxygen atoms of catempo^- and pyridyl nitrogen atom of 4,4'-bpy with Cu-O distances of 1.945(4)–1.964(4) Å and Cu-N distance of 2.121(4) Å, respectively, to form a distorted square pyramidal geometry. The copper atoms lie on the basal O_4 plane toward the axial nitrogen atom by 0.20 Å. The $\text{Cu1}'\cdots\text{Cu1-N2}$ angle is 176.34(12)°, resulting in a nearly linear chain structure in the crystal. In the crystal, methanol molecule is included and formed hydrogen-bonding with carboxylate-oxygen atom, as shown in Figure 9.

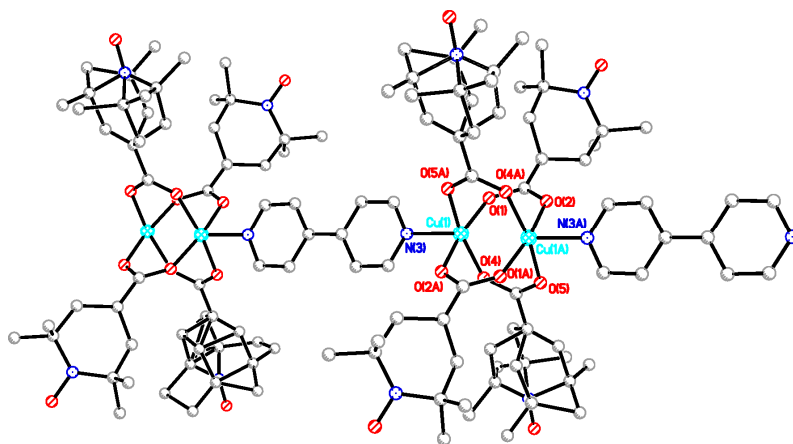


Figure 8. Perspective view of chain molecule for $[\text{Cu}_2(\text{catempo})_4(4,4'\text{-bpy})]_n$ (**9**). Hydrogen atoms are omitted for clarity.

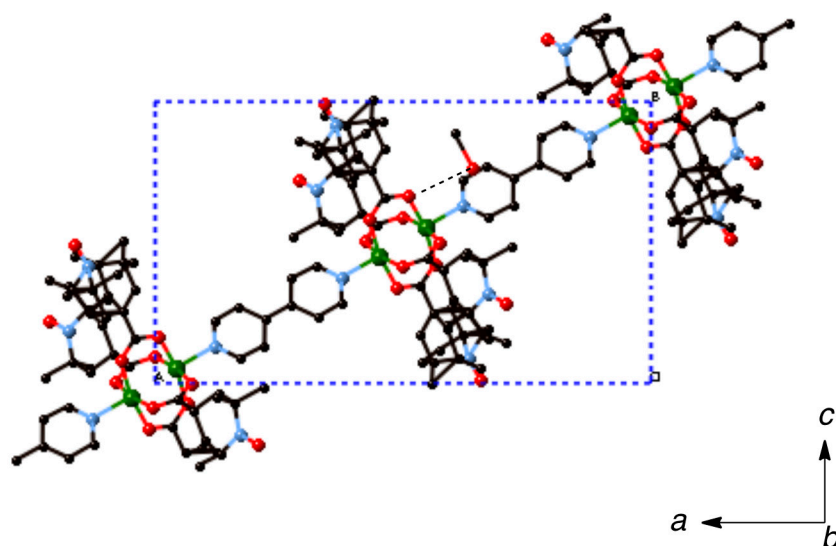


Figure 9. Packing diagram of $[\text{Cu}_2(\text{catempo})_4(4,4'\text{-bpy})]_n$ (**9**). Hydrogen atoms are omitted for clarity. Dotted line denotes the hydrogen bonding.

The chain adduct of $\text{Cu}_2(\text{catempo})_4$ system with dpe ligand, $[\text{Cu}_2(\text{catempo})_4(\text{dpe})]_n$ (**10**), crystallizes in the tetragonal system. Selected good crystals were subjected to the X-ray crystal structure analysis. Nonetheless, these crystals easily decomposed and provided only poor crystallographic

data. A perspective view of the molecular structure of **10** is depicted in Figure 10. The two copper atoms are equatorially linked by the four bridging carboxylate radicals (catempo⁻), because of the crystallographic symmetry and the pyridine rings of bpe are axially coordinated. The molecular structure of **10** consists of alternating linking of dinuclear Cu₂(catempo)₄ cluster and bpe ligand to construct a crystallographically linear chain molecule with Cu'...Cu-N angle of 180°.

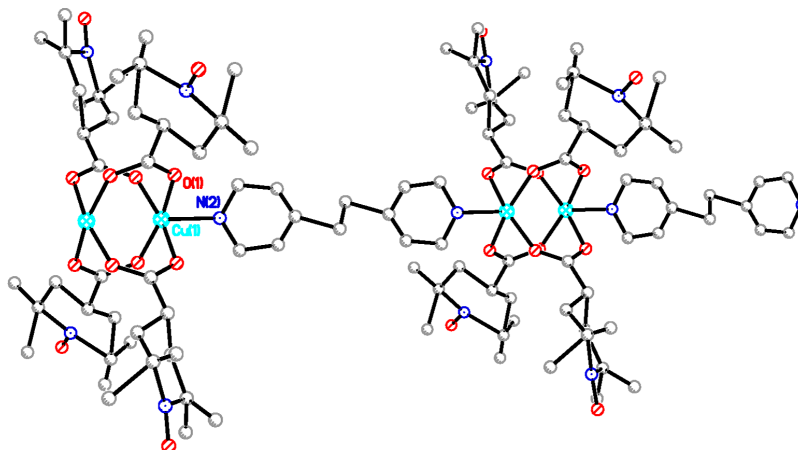


Figure 10. Perspective view of chain molecule for [Cu₂(catempo)₄(bpe)]_n (**10**). Hydrogen atoms are omitted for clarity.

In the crystal, water molecules are included and formed hydrogen-bondings with nitrogen atom of bpe ligand, as shown in Figure 11.

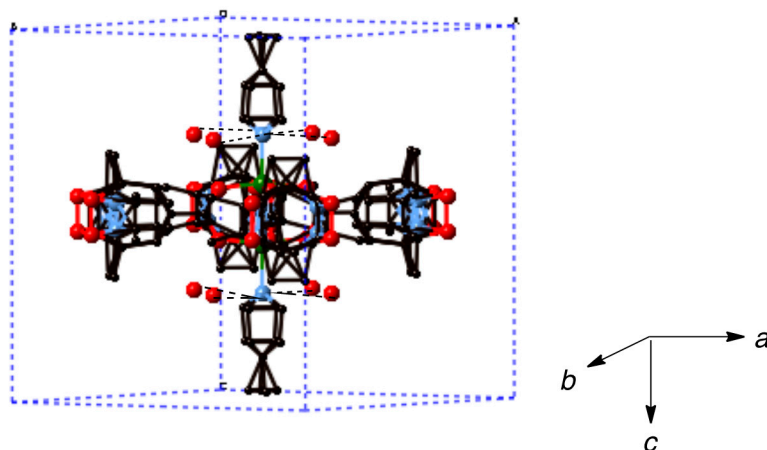


Figure 11. Packing diagram of [Cu₂(catempo)₄(bpe)]_n (**10**). Hydrogen atoms are omitted for clarity. Dotted lines denote the hydrogen bondings.

From the crystal structures, it was found out that the present linking ligands can work as a connector to assemble the copper-acetate type dinuclear clusters with four radical spins. The pds linking ligand was expected to form a chiral chain for constructing chiral magnetic materials. However, we could not find out the way to isolate such species in the present study. Further studies are needed to obtain a chiral chain compound.

2.5. Magnetic Data of One-Dimensional Coordination Polymers.

The magnetic properties for the chain compounds **6** and **9** are displayed in Figure 12, as the temperature variations of effective magnetic moment (μ_{eff}) and susceptibility (χ_{M}) as representative examples. The present complexes exhibit room-temperature magnetic moments at around $4 \mu_{\text{B}}$ per mole of the dinuclear unit, as shown in Table 7. In general, the observed values of effective magnetic moments tend to be a little lower than the theoretical value. The calculated spin-only value is $4.24 \mu_{\text{B}}$ for non-interacting six $1/2$ spin that was sourced from the dinuclear copper core with four nitroxide radicals. When cooling, the magnetic moments steadily decrease from 300 to ca. 15 K, and then abruptly diminish to a value of approximately $3\text{--}3.5 \mu_{\text{B}}$ per mole of the dinuclear unit at 4.5 K. Overall, each chain adduct shows a similar pattern of magnetic moment decreasing with lowering of temperature, suggesting that the magnetic behavior is antiferromagnetic as a whole. Therefore, the magnetic property of present complexes was described by the equation (Equation (1)) based on a chain model consisting of a dinuclear copper(II) unit and four radicals,

$$\chi_{\text{M}} = (2Ng^2\beta^2/kT) [3 + \exp(-2J/kT)]^{-1} + C/(T - \theta) + 2N\alpha \quad (1)$$

in which J is the exchange integral for the two copper(II) ions, θ is the Weiss temperature to account for the interaction between the radical and copper(II) ion, radical-radical, and/or the dinuclear cluster-dinuclear cluster interaction, and the other symbols have their usual meanings [14,18]. The best fitting parameters are shown in Table 7. The J values of the chain adducts are in the range of $-125\text{--}-245 \text{ cm}^{-1}$ for the caproxy and catempo systems, confirming that the copper(II) ions are coupled antiferromagnetically. These coupling constants are comparable to those of the parent complexes as well as the copper(II) carboxylate clusters [3–7]. The interpretation of small negative θ values can be deduced for the radical and copper(II) ion, radical-radical, and/or the dinuclear cluster-dinuclear cluster interaction. In the various complexes of paddle-wheel type dinuclear copper(II) carboxylates with axially-coordinated nitroxide radicals [14,25,26], the copper atoms are normally found to weakly interact with the radicals in antiferromagnetic fashion. The interaction between dinuclear clusters via the linking N,N' -bidentate ligands is weak probably because of the long distance between the dinuclear clusters. Sarma et al. have reported chain systems for the paddle wheel unit of $[\text{Cu}_2(o\text{-NO}_2\text{-C}_6\text{H}_4\text{COO})_4(\text{BPNO})_2]$ with two kinds of spacer ligands ($4,4'$ -bipyridyl- N,N' -dioxide and $2,2'$ -bipyridyl- N,N' -dioxide) and pointed out no discernible interaction between the units [39].

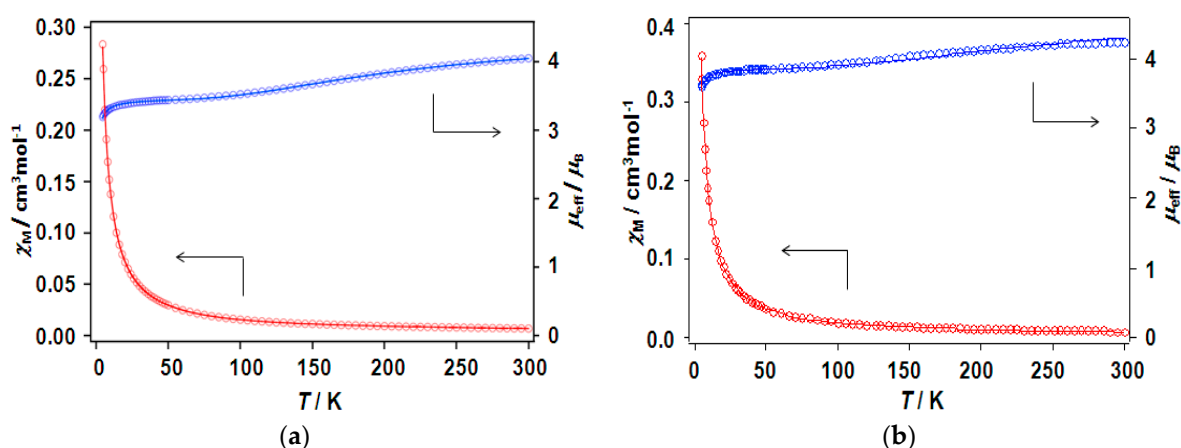


Figure 12. Temperature dependence of magnetic susceptibilities (red circles) and magnetic moments (blue circle) of chain compounds (a) $[\text{Cu}_2(\text{caproxy})_4(\text{pds})]_n$ (**6**) and (b) $[\text{Cu}_2(\text{catempo})_4(4,4'\text{-bpy})]_n$ (**9**).

Table 7. Magnetic data of the chain compounds.

Complex (Linking Ligand)	μ_{eff} at 300 K (μ_B)	g	J (cm^{-1})	θ (K)	C ($\text{cm}^3\text{Kmol}^{-1}$)
1	4.03	2.20	−166	−2.90	1.56
2	3.92	2.12	−173	−1.20	1.49
3 (4,4′-bpy)	4.04	2.34	−163	−1.60	1.48
4 (bpe)	4.31	2.10	−178	−2.00	2.00
5 (bpel)	3.87	2.10	−186	−1.80	1.51
6 (pds)	4.24	2.10	−176	−0.76	1.88
7 (dabco)	4.02	2.27	−167	−2.40	1.51
8 (pyz)	3.85	2.12	−206	−2.30	1.51
9 (4,4′-bpy)	4.05	2.23	−149	−0.82	1.49
10 (bpe)	3.96	2.10	−167	−2.80	1.56
11 (bpel)	3.84	2.10	−125	−0.87	1.40
12 (pds)	4.27	2.20	−146	−1.80	1.69
13 (dabco)	3.62	2.10	−245	−1.80	1.40

3. Materials and Methods

All of the chemicals were commercial products and were used as supplied. The parent dinuclear carboxylates, $[\text{Cu}_2(\text{caproxy})_4(\text{H}_2\text{O})_2]$ (1) and $[\text{Cu}_2(\text{catempo})_4(\text{H}_2\text{O})_2]$ (2) were prepared according to a method reported in the literature [18]. The crude products were recrystallized once from distilled acetonitrile, filtered and dried in vacuo above P_2O_5 prior to subsequent synthesis. Anal. Found for 1: C, 47.58; H, 7.23; N, 5.67%. Calcd. for $\text{C}_{36}\text{H}_{60}\text{Cu}_2\text{N}_4\text{O}_{12}\cdot 2.5\text{H}_2\text{O}$: C, 47.36; H, 7.18; N, 6.14%. Found for 2: C, 50.25; H, 7.51; N, 6.22%. Calcd. for $\text{C}_{40}\text{H}_{68}\text{Cu}_2\text{N}_4\text{O}_{12}\cdot 2\text{H}_2\text{O}$: C, 50.04; H, 7.56; and, N, 5.84%.

Synthesis of $[\text{Cu}_2(\text{caproxy})_4(4,4'\text{-bpy})]_n\cdot 0.5n\text{H}_2\text{O}$ (3). To an acetonitrile solution of 4,4′-bpy (5.8 mg, 0.037 mmol), an acetonitrile solution of 1 (30.2 mg, 0.033 mmol) was added, forming a light-green precipitate. After the reaction mixture was stirred for 1h, the mixture was left for one day. The solid was filtered off and desiccated in vacuo. Yield: 30.8 mg, 90% (based on the parent complex). Found C 53.57, H 7.03, N 7.73%. Calcd for $\text{C}_{46}\text{H}_{68}\text{Cu}_2\text{N}_6\text{O}_{12}\cdot 0.5\text{H}_2\text{O}$: C 53.48, H 6.73, N 8.13%.

Synthesis of $[\text{Cu}_2(\text{caproxy})_4(\text{bpe})]_n\cdot 0.5n\text{CH}_3\text{CN}\cdot 2n\text{H}_2\text{O}$ (4). Compound 4 was prepared as for 3 using bpe (5.8 mg, 0.031 mmol) and 1 (25.8 mg, 0.029 mmol). Yield: 23.4 mg, 77.9% (based on the parent complex). Found C 52.84, H 6.88, N 8.09%. Calcd for $\text{C}_{48}\text{H}_{72}\text{Cu}_2\text{N}_6\text{O}_{12}\cdot 0.5\text{CH}_3\text{CN}\cdot 2\text{H}_2\text{O}$: C 53.08, H 7.05, N 8.21%.

Synthesis of $[\text{Cu}_2(\text{caproxy})_4(\text{bpel})]_n\cdot 0.5n\text{H}_2\text{O}$ (5). Compound 5 was prepared as for 3 using bpel (5.8 mg, 0.032 mmol) and 1 (25.2 mg, 0.028 mmol). Yield: 27.0 mg, 92.2% (based on the parent complex). Found C 54.08, H 6.25, N 7.97%. Calcd for $\text{C}_{48}\text{H}_{70}\text{Cu}_2\text{N}_6\text{O}_{12}\cdot 0.5\text{H}_2\text{O}$: C 54.43, H 6.76, N 7.93%.

Synthesis of $[\text{Cu}_2(\text{caproxy})_4(\text{pds})]_n\cdot 0.5n\text{CH}_3\text{CN}\cdot 2n\text{H}_2\text{O}$ (6). Compound 6 was prepared as for 3 using pds (8.1 mg, 0.037 mmol) and 1 (30.8 mg, 0.034 mmol). Yield: 29.8 mg, 80.4% (based on the parent complex). Found C 49.10, H 6.00, N 8.38%. Calcd for $\text{C}_{46}\text{H}_{68}\text{Cu}_2\text{N}_6\text{O}_{12}\text{S}_2\cdot 0.5\text{CH}_3\text{CN}\cdot 2\text{H}_2\text{O}$: C 49.31, H 6.47, N 7.95%. X-ray quality crystals were grown by slow diffusion process using H-formed tube at ambient temperature.

Synthesis of $[\text{Cu}_2(\text{caproxy})_4(\text{dabco})]_n$ (7). Compound 7 was prepared as for 3 using dabco (4.8 mg, 0.043 mmol) and 1 (30.2 mg, 0.033 mmol). Yield: 29.2 mg, 89.2% (based on the parent complex). Found C 50.99, H 6.95, N 8.59%. Calcd for $\text{C}_{42}\text{H}_{72}\text{Cu}_2\text{N}_6\text{O}_{12}$: C 51.47, H 7.40, N 8.57%.

Synthesis of $[\text{Cu}_2(\text{caproxy})_4(\text{pyz})]_n\cdot 2n\text{H}_2\text{O}$ (8). Compound 8 was prepared as for 3 using pyz (3.4 mg, 0.042 mmol) and 1 (25.6 mg, 0.028 mmol). Yield: 16.1 mg, 60% (based on the parent complex). Found C 48.72, H 6.67, N 8.37%. Calcd for $\text{C}_{40}\text{H}_{64}\text{Cu}_2\text{N}_6\text{O}_{12}\cdot 2\text{H}_2\text{O}$: C 48.82, H 6.96, N 8.54%.

Synthesis of $[\text{Cu}_2(\text{catempo})_4(4,4'\text{-bpy})]_n$ (9). To an acetonitrile solution of 4,4′-bpy (6.8 mg, 0.044 mmol), an acetonitrile solution of 2 (40 mg, 0.042 mmol) was added, forming a light-green

precipitate. After the reaction mixture was stirred for 1h, the mixture was left for one day. The solid was filtered off and was desiccated in vacuo. Yield: 40.0 mg, 88.9% (based on the parent complex). Found C 55.83, H 6.59, N 7.73%. Calcd for $C_{50}H_{76}Cu_2N_6O_{12}$: C 55.59, H 7.09, N 7.78%. X-ray quality crystals were grown by slow diffusion process at ambient temperature.

Synthesis of $[Cu_2(\text{catempo})_4(\text{bpe})]_n \cdot 1.5nH_2O$ (10). Compound 10 was prepared as for 9 using bpe (8.0 mg, 0.043 mmol) and 2 (40.1 mg, 0.042 mmol). Yield: 40.4 mg, 87.3% (based on the parent complex). Found C 55.02, H 7.20, N 7.75%. Calcd for $C_{52}H_{80}Cu_2N_6O_{12} \cdot 1.5H_2O$: C 55.01, H 7.37, N 7.40%. X-ray quality crystals were grown by slow diffusion process at ambient temperature.

Synthesis of $[Cu_2(\text{catempo})_4(\text{bpel})]_n \cdot nCH_3CN \cdot 0.5nH_2O$ (11). Compound 11 was prepared as for 9 using bpel (7.9 mg, 0.043 mmol) and 2 (40.2 mg, 0.042 mmol). Yield: 26.0 mg, 56.1% (based on the parent complex). Found C 55.77, H 6.84, N 8.69%. Calcd for $C_{52}H_{78}Cu_2N_6O_{12} \cdot CH_3CN \cdot 0.5H_2O$: C 56.09, H 7.15, N 8.48%.

Synthesis of $[Cu_2(\text{catempo})_4(\text{pds})]_n \cdot 0.5nCH_3CN$ (12). Compound 12 was prepared as for 9 using pds (7.0 mg, 0.032 mmol) and 2 (30.0 mg, 0.031 mmol). Yield: 26.8 mg, 74.9% (based on the parent complex). Found C 53.03, H 6.23, N 7.57%. Calcd for $C_{50}H_{76}Cu_2N_6O_{12}S_2 \cdot 0.5CH_3CN$: C 52.58, H 6.71, N 7.82%.

Synthesis of $[Cu_2(\text{catempo})_4(\text{dabco})]_n \cdot nH_2O$ (13). Compound 13 was prepared as for 9 using dabco (3.7 mg, 0.033 mmol) and 2 (30.0 mg, 0.031 mmol). Yield: 26.5 mg, 81.8% (based on the parent complex). Found C 52.18, H 7.60, N 8.12%. Calcd for $C_{46}H_{80}Cu_2N_6O_{12} \cdot H_2O$: C 52.41, H 7.84, N 7.97%.

Elemental analyses for C, H, and N were performed using a Thermo-Finnigan FLASH EA1112 series CHNO-S analyzer. Infrared spectra were measured with a JASCO MFT-2000 FT-IR Spectrophotometer in the 4000–600 cm^{-1} region. Solution spectra (in CH_3OH) were recorded on a Shimadzu UV-vis-NIR Recording Spectrophotometer Model UV-3100 in the 200–1000 nm region. Diffused reflectance spectra were measured with a Shimadzu UV-vis-NIR Recording Spectrophotometer Model UV-3100 that was equipped with an integrating sphere in the 200–2000 nm region. Magnetic susceptibilities were measured with a Quantum Design MPMS-XL7 SQUID susceptometer over a temperature range of 4.5–300 K.

Single-crystal diffraction data were measured on a Bruker Smart APEX CCD diffractometer equipped with a graphite crystal and incident beam monochromator using Mo $K\alpha$ radiation ($\lambda = 0.71073 \text{ \AA}$). The structure was solved by direct methods, and was refined by full-matrix least-squares methods. The hydrogen atoms were inserted at their calculated positions and fixed there. All of the calculations were carried out utilizing the SHELXTL software package [40]. Crystallographic data have been deposited with Cambridge Crystallographic Data Centre: Deposit numbers CCDC-1836763-1836765 and 1836862. Copies of the data can be obtained free of charge via <http://www.ccdc.cam.ac.uk/conts/retrieving.html> (or from the Cambridge Crystallographic Data Centre, 12, Union Road, Cambridge, CB2 1EZ, UK; Fax: +44 1223 336033; e-mail: deposit@ccdc.cam.ac.uk).

4. Conclusions

In this study, two dinuclear copper(II) complexes of free radical carboxylic acid, $[Cu_2(\text{caproxy})_4(H_2O)_2]$ and $[Cu_2(\text{catempo})_4(H_2O)_2]$, have been evolved into coordination polymer by using six types of N,N' -bidentate ligands. Eleven chain adducts, formulated as $[Cu_2(\text{caproxy})_4(L)]_n$ ($L = 4,4'$ -bpy (3), bpe (4), bpel (5), pds (6), dabco (7), pyz (8)) and $[Cu_2(\text{catempo})_4(L)]_n$ ($L = 4,4'$ -bpy (9), bpe (10), bpel (11), pds (12), dabco (13)), were prepared in satisfactory yield as well as characterized. The crystal structures of $[Cu_2(\text{caproxy})_4(\text{pds})]_n$, $[Cu_2(\text{catempo})_4(4,4'\text{-bpy})]_n$ and $[Cu_2(\text{catempo})_4(\text{bpe})]_n$ revealed that the bridging carboxylate radicals (caproxy $^-$ and catempo $^-$) are integrated in the dinuclear copper core, thus configuring a 'paddle-wheel' type structure, and each dinuclear cluster is connected by the linking ligand (pds, 4,4'-bpy, and bpe) to form a chain molecule. For the other complexes, a chain structure with an alternated arrangement of the $Cu_2(\text{caproxy})_4$ or $Cu_2(\text{catempo})_4$ dinuclear unit and the N,N' -bidentate ligands can be proposed based on the analytical data, infrared and electronic

spectra, as well as the bridging nature of the N,N' -bidentate ligands. The magnetic interaction via the N,N' -bidentate spacer ligand was found to be generally weak and antiferromagnetic. Although, the present linking ligands did not occur a stronger interaction between the copper(II) clusters, it is important to find out that several linking ligands can work connect the clusters with multiple radicals to assemble the spins to construct magnetic materials as the first step.

Author Contributions: M.M. conceived and designed the experiments, analyzed the data, and wrote the paper; R.I. performed the experiments and wrote the paper; S.M., C.N., R.H., K.Y., and M.F. performed the experiments; D.Y. performed the crystallographic work; M.H. wrote the paper.

Acknowledgments: The present work was partially supported by Grant-in-Aid for Scientific Research Nos. 16K05722 and 17K05820 from the Ministry of Education, Culture, Sports, Science and Technology (MEXT, Japan) and the MEXT-Supported Program for the Strategic Research Foundation at Private Universities, 2010–2014.

Conflicts of Interest: The authors declare no conflict of interest.

References

1. Van Niekerk, J.N.; Schoening, F.R. A New Type of Copper Complex as found in the Crystal Structure of Cupric Acetate, $\text{Cu}_2(\text{CH}_3\text{COO})_4 \cdot 2\text{H}_2\text{O}$. *Acta Crystallogr.* **1953**, *6*, 227–232. [[CrossRef](#)]
2. Bleaney, B.; Bowers, K.D. Anomalous paramagnetism of copper acetate. *Proc. R. Soc. Lond. A* **1952**, *214*, 451–465. [[CrossRef](#)]
3. Doedens, R.J. Structure and Metal-Metal Interactions in Copper(II) Carboxylate Complexes. *Prog. Inorg. Chem.* **1976**, *21*, 209–231.
4. Melnik, M. Study of the relation between the structural data and magnetic interaction in oxo-bridged binuclear copper(II) compounds. *Coord. Chem. Rev.* **1982**, *42*, 259–293. [[CrossRef](#)]
5. Kato, M.; Muto, Y. Factors affecting the magnetic properties of dimeric copper(II) complexes. *Coord. Chem. Rev.* **1988**, *92*, 45–83. [[CrossRef](#)]
6. Sundberg, M.R.; Uggla, R.; Melnik, M. Comparison of the structural parameters in copper(II) acetate-type dimers containing distorted square pyramidal Cu_4O and CuO_4N chromophores. *Polyhedron* **1996**, *15*, 1157–1163. [[CrossRef](#)]
7. Mikuriya, M. Copper(II) Acetate as a Motif of Metal-Assembled complexes. *Bull. Jpn. Soc. Coord. Chem.* **2008**, *52*, 17–28. (In Japanese) [[CrossRef](#)]
8. Mikuriya, M.; Kida, S.; Ueda, I.; Tokii, T.; Muto, Y. The Crystal Structure and Magnetic Property of Di- μ -propionato- O,O' -bis[N - p -tolylsalicylideneaminatocopper(II)]. *Bull. Chem. Soc. Jpn.* **1977**, *50*, 2464–2470. [[CrossRef](#)]
9. Nakashima, M.; Mikuriya, M.; Muto, Y. Structural, Magnetic and IR Spectroscopic Characterization of Dinuclear Copper(II) Trichloroacetate Adduct with Benzonitrile. Nature of the Copper(II)-benzonitrile Bond. *Bull. Chem. Soc. Jpn.* **1985**, *58*, 968–973. [[CrossRef](#)]
10. Mikuriya, M.; Nukada, R.; Morishita, H.; Handa, M. Chain Compounds Formed by the Reaction of Copper(II) Carboxylate $[\text{Cu}_2(\text{O}_2\text{CR})_4]$ ($\text{R} = \text{C}(\text{CH}_3)_3, \text{CCl}_3$) and Bridging Ligand L ($\text{L} = \text{Pyrazine}, 4,4'$ -Bipyridine, and 1,4-Diazabicyclo[2.2.2]octane). *Chem. Lett.* **1995**, *24*, 617–618. [[CrossRef](#)]
11. Mikuriya, M.; Azuma, H.; Nukada, R.; Handa, M. Synthesis, X-Ray Structures, and Magnetic Properties of $[\text{Cu}_2(\text{piv})_4(\text{Et}_3\text{N})_2]$ and $[\text{Cu}_6(\text{piv})_6(\text{EtO})_6]$ (Hpiv = Pivalic Acid): Role of Base for Dinuclear Adduct and Oligonuclear Formation. *Chem. Lett.* **1999**, *28*, 57–58. [[CrossRef](#)]
12. Nukada, R.; Mori, W.; Takamizawa, S.; Mikuriya, M.; Handa, M.; Naono, H. Microporous Structure of a Chain Compound of Copper(II) Benzoate Bridged by Pyrazine. *Chem. Lett.* **1999**, *28*, 367–368. [[CrossRef](#)]
13. Matsushima, H.; Koikawa, M.; Nukada, R.; Mikuriya, M.; Tokii, T. Structural Characterization and Magnetic Properties of Triply Carboxylato-Bridged Dinuclear Copper(II) Complexes. *Bull. Chem. Soc. Jpn.* **1999**, *72*, 1025–1035. [[CrossRef](#)]
14. Mikuriya, M.; Azuma, H.; Nukada, R.; Sayama, Y.; Tanaka, K.; Lim, J.-W.; Handa, M. Antiferromagnetic Adducts of Copper(II) Propionate with Pyridyl Nitronyl Nitroxides. *Bull. Chem. Soc. Jpn.* **2000**, *73*, 2493–2498. [[CrossRef](#)]
15. Mikuriya, M.; Azuma, H.; Handa, M. Coordination Polymers of Copper(II) and Copper(I) Trifluoroacetates with Pyrazine. *Mol. Cryst. Liq. Cryst.* **2000**, *342*, 205–210. [[CrossRef](#)]

16. Nukada, R.; Mikuriya, M.; Yamashita, A.; Handa, M. Mononuclear and Polynuclear Chain Compounds of Copper(II) Pivalate with *N,N'*-Didentate Ligands. In *Challenges for Coordination Chemistry in the New Century*; Melnik, M., Sirota, A., Eds.; Slovak Technical University Press: Bratislava, Slovakia, 2001; pp. 83–88.
17. Mikuriya, M.; Azuma, H.; Handa, M. Coordination Polymers of Copper(II) Propionate with Linking Ligands. *Mol. Cryst. Liq. Cryst.* **2002**, *379*, 205–210. [[CrossRef](#)]
18. Mikuriya, M.; Azuma, H.; Sun, J.; Yoshioka, D.; Handa, M. Dinuclear Copper(II) Complexes of Free Radical Carboxylic Acids. *Chem. Lett.* **2002**, *31*, 608–609. [[CrossRef](#)]
19. Horikoshi, R.; Mikuriya, M. One-Dimensional Coordination Polymers from the Self-Assembly of Copper(II) Carboxylates and 4,4'-Dithiobis(pyridine). *Bull. Chem. Soc. Jpn.* **2005**, *78*, 827–834. [[CrossRef](#)]
20. Lorinc, S.; Koman, M.; Melnik, M.; Mikuriya, M. Mono-, di- and polymeric copper(II) complexes with diclofenic acid (nsaid drug), structures, spectral and magnetic properties. In *Advances in Coordination, Bioinorganic and Inorganic Chemistry*; Melnik, M., Sima, J., Tatarko, M., Eds.; Slovak Technical University Press: Bratislava, Slovakia, 2005; pp. 176–186.
21. Mikuriya, M.; Yano, M.; Takahashi, N.; Yoshioka, D.; Tanaka, H.; Handa, M. Synthesis and Crystal Structure of a Chain Complex of Copper(II) Pivalate and 1,2-Bis(4-pyridyl)ethane in Relation to Adsorption Property for N₂. *X-ray Struct. Anal. Online* **2015**, *31*, 47–48. [[CrossRef](#)]
22. Mikuriya, M.; Yano, M.; Takahashi, N.; Yoshioka, D.; Tanaka, H.; Handa, M. Synthesis, crystal structure, magnetic property, and N₂-gas-adsorption property of chain compounds of dinuclear copper(II) pivalate with *N,N'*-bidentate ligands. In Proceedings of the 2nd International Porous and Powder Materials Symposium and Exhibition PPM 2015, Izmir, Turkey, 15–18 September 2015; Ozdemir, S.K., Polat, M., Tanoglu, M., Eds.; The Organizing Committee of The International Porous and Power Materials Symposium and Exhibition: Izmir, Turkey, 2015; pp. 72–76.
23. Nukada, R.; Mikuriya, M.; Handa, M.; Naono, H. Hydrophobic micropore in a chain compound of dinuclear copper(II) benzoate with pyrazine—Adsorption properties for N₂, CCl₄, H₂O, CO₂, and CH₃CN. In Proceedings of the 2nd International Porous and Powder Materials Symposium and Exhibition PPM 2015, Izmir, Turkey, 15–18 September 2015; Ozdemir, S.K., Polat, M., Tanoglu, M., Eds.; The Organizing Committee of The International Porous and Power Materials Symposium and Exhibition: Izmir, Turkey, 2015; pp. 77–81.
24. Mikuriya, M.; Yamakawa, C.; Tanabe, K.; Yoshioka, D.; Mitsuhashi, R.; Tanaka, H.; Handa, M. Synthesis, crystal structure, magnetic property, and N₂-gas-adsorption property of dinuclear copper(II) 3,4,5-trimethoxybenzoate. In Proceedings of the 3rd International Porous and Powder Materials Symposium and Exhibition PPM 2017, Izmir, Turkey, 12–15 September 2017; Duvarei, O.C., Polat, M., Tanoglu, M., Eds.; The Organizing Committee of The 3rd International Porous and Power Materials Symposium and Exhibition: Izmir, Turkey, 2017; pp. 451–455.
25. Chung, Y.-H.; Wei, H.-H.; Lee, G.-H.; Wang, Y. Magneto-structural correlation of dimeric copper(II) carboxylates with pyridyl-substituted nitronyl nitroxides. *Inorg. Chim. Acta* **1999**, *293*, 30–36. [[CrossRef](#)]
26. Chung, Y.-H.; Wei, H.-H. A novel chain complex of dicopper(II) trimethylacetate linked by pyridyl nitronyl nitroxide. *Inorg. Chem. Commun.* **1999**, *2*, 269–271. [[CrossRef](#)]
27. Dasna, I.; Golhen, S.; Ouahab, L.; Pena, O.; Daro, N.; Sutter, J.P. A dimeric Cu(II) acetate complex containing axially coordinated *p*-pyridyl nitroxide radicals: [Cu^{II}(CH₃COO)₂(NITpPy)]₂. *New J. Chem.* **2000**, *24*, 903–906. [[CrossRef](#)]
28. Del Sesto, R.E.; Arif, A.M.; Miller, J.S. Copper(II) Benzoate Nitroxide Dimers and Chains: Structure and Magnetic Studies. *Inorg. Chem.* **2000**, *39*, 4894–4902. [[CrossRef](#)] [[PubMed](#)]
29. Nakamoto, K. *Infrared and Raman Spectra of Inorganic and Coordination Compounds, Part B*, 6th ed.; John Wiley & Sons: Hoboken, NJ, USA, 2009; pp. 64–67. ISBN 978-0-471-74493-1.
30. Agarwal, R.K.; Singh, L.; Sharma, D.K.; Singh, R. Spectral and Thermal Investigations of Some Oxovanadium(IV) Complexes of Hydrazones of Isonicotinic Acid Hydrazide. *Turk. J. Chem.* **2005**, *29*, 309–316.
31. Marques, L.F.; Marinho, M.V.; Correa, C.C.; Speziali, N.L.; Diniz, R.; Machado, F.C. One-dimensional Copper(II) Coordination Polymers Based on Carboxylate Anions and Rigid Pyridyl-Donor Ligands. *Inorg. Chim. Acta* **2011**, *368*, 242–246. [[CrossRef](#)]

32. Marinho, M.V.; Yoshida, M.I.; Guedes, K.J.; Krambrock, K.; Bortoluzzi, A.J.; Horner, M.; Machado, F.C.; Teles, W.M. Synthesis, Crystal Structure, and Spectroscopic Characterization of trans-Bis[(μ -1,3-bis(4-pyridyl)propane)(μ -(3-thiopheneacetate-O))(3-thiopheneacetate-O)]dicopper(II), $\{[\text{Cu}_2(\text{O}_2\text{CCH}_2\text{C}_4\text{H}_3\text{S})_4-\mu\text{-(BPP)}_2]\}_n$: From a Dinuclear Paddle-Wheel Copper(II) Unit to a 2-D Coordination Polymer Involving Monoatomic Carboxylate Bridges. *Inorg. Chem.* **2004**, *43*, 1539–1544. [[CrossRef](#)] [[PubMed](#)]
33. Teles, W.M.; Fernandes, N.G.; Abras, A.; Filgueiras, C.A.L. The Chemical Behavior of di(2-pyridyl)sulphide, dps. Crystal and Molecular Structure of μ -di(2-pyridyl)sulphidebis(*trans*-dichlorotriethylphosphineplatinum(II)), $[\{\text{Pt}(\text{PEt}_3\text{Cl}_2)_2\mu\text{-dps}]$ and its Reactivity Towards Stannylated Species. *Transit. Met. Chem.* **1999**, *24*, 321–325. [[CrossRef](#)]
34. Marzocchi, M.P.; Sbrana, G.; Zerbi, G. Structure and Fundamental Vibrations of Cage Molecules. I. 1,4-Diazabicyclo[2.2.2]octane. *J. Am. Chem. Soc.* **1965**, *87*, 1429–1432. [[CrossRef](#)]
35. Murakami, Y.; Sakata, K. *Kireto Kagaku*; Ueno, K., Ed.; Nankodo: Tokyo, Japan, 1976; Volume 1, pp. 91–396. (In Japanese)
36. Capiomont, P.A.; Lajzrowicz-Bonneteau, J. Etude du Radical Nitroxyde Tétraméthyl-2,2,6,6 Piperidine-1 Oxyle-1 ou 'Tanane'. II. Affinement de la Structure Cristallographique de la Forme Quadratique Désordonnée. *Acta Crystallogr. Sect. B* **1974**, *30*, 2160–2166. [[CrossRef](#)]
37. Horikoshi, R.; Mikuriya, M. Self-Assembly of Repeated Rhomboidal Coordination Polymers from 4,4'-Dipyridyl Disulfide and ZnX_2 Salts ($\text{X} = \text{SCN}, \text{NO}_3, \text{ClO}_4$). *Cryst. Growth Des.* **2005**, *5*, 223–230. [[CrossRef](#)]
38. Horikoshi, R.; Mochida, T.; Kurihara, M.; Mikuriya, M. Supramolecular Isomerism in Self-Assembled Complexes from 4,4'-Dipyridyl Disulfide and $\text{M}(\text{hfac})_2$: Coordination Polymers ($\text{M} = \text{Mn}$) and Metallamacrocycles ($\text{M} = \text{Co}, \text{Ni}$). *Cryst. Growth Des.* **2005**, *5*, 243–249. [[CrossRef](#)]
39. Sarma, R.; Boudalis, K.; Baruah, J.B. Aromatic N-oxide Bridged Copper(II) Coordination Polymers: Synthesis, Characterization and Magnetic Properties. *Inorg. Chim. Acta* **2010**, *363*, 2279–2286. [[CrossRef](#)]
40. Sheldrick, G.M. A short history of SHELX. *Acta Crystallogr. Sect. A* **2008**, *64*, 112–122. [[CrossRef](#)] [[PubMed](#)]



© 2018 by the authors. Licensee MDPI, Basel, Switzerland. This article is an open access article distributed under the terms and conditions of the Creative Commons Attribution (CC BY) license (<http://creativecommons.org/licenses/by/4.0/>).